sustainability

MDPI

Article

Recent Oasis Dynamics and Ecological Security in the Tarim River Basin, Central Asia

Qifei Zhang [1,2], Congjian Sun [1,2,*], Yaning Chen [2,*], Wei Chen [1], Yanyun Xiang [2,3], Jiao Li [1] and Yuting Liu [2,4]

[1] School of Geographical Sciences, Shanxi Normal University, Taiyuan 030031, China; zhangqifei15@mails.ucas.ac.cn (Q.Z.); wan_xin_chen@126.com (W.C.); lijiao@itpcas.ac.cn (J.L.)
[2] State Key Laboratory of Desert and Oasis Ecology, Xinjiang Institute of Ecology and Geography, Chinese Academy of Sciences, Urumqi 830011, China; xiangyanyun18@mails.ucas.ac.cn (Y.X.); xiaoxiao861211@163.com (Y.L.)
[3] School of Public Administration, Shanxi University of Finance and Economics, Taiyuan 030006, China
[4] School of Life and Geography, Kashi University, Kashi 844000, China
* Correspondence: suncongjian@sina.com (C.S.); chenyn@ms.xjb.ac.cn (Y.C.); Tel.: +86-351-205-1801 (C.S.); +86-991-782-3169 (Y.C.)

Abstract: As an important agricultural and gathering area in arid inland areas of China, the ecological environments of oasis areas are more sensitive to regional climate change and human activities. This paper investigates the dynamic evolution of the oases in the Tarim River basin (TRB) and quantitatively evaluates the regional ecological security of oases via a remote sensing ecological index (RSEI) and net primary productivity (NPP) through the Carnegie–Ames–Stanford approach (CASA) from 2000 to 2020. The results indicate that the total plain oasis area in the TRB during the study period experienced an increasing trend, with the area expanding by 8.21%. Specifically, the artificial oases (cultivated and industrial land) showed a notable increase, whereas the natural oases (forests and grassland) exhibited an apparent decrease. Among the indictors of oasis change, the Normalised Difference Vegetation Index (NDVI) increased from 0.13 to 0.16, the fraction of vegetation cover (FVC) expanded by 36.79%, and NPP increased by 31.55%. RSEI changes indicated that the eco-environment of the TRB region went from poor grade to general grade; 69% of the region's eco-environment improved, especially in western mountainous areas, and less than 5% of the regions' eco-ecological areas were degraded, mainly occurring in the desert-oasis ecotone. Changes in land- use types of oases indicated that human activities had a more significant influence on oases expansion than natural factors. Our results have substantial implications for environment protection and sustainable economic development along the Silk Road Economic Belt.

Keywords: oasis dynamics; Normalised Difference Vegetation Index (NDVI); fraction of vegetation cover (FVC); net primary productivity (NPP); remote sensing ecological index (RSEI); Tarim River basin (TRB)

check for updates

Citation: Zhang, Q.; Sun, C.; Chen, Y.; Chen, W.; Xiang, Y.; Li, J.; Liu, Y. Recent Oasis Dynamics and Ecological Security in the Tarim River Basin, Central Asia. *Sustainability* **2022**, *14*, 3372. https://doi.org/10.3390/su14063372

Academic Editor: Daniela Smiraglia

Received: 5 February 2022
Accepted: 11 March 2022
Published: 13 March 2022

1. Introduction

Oases are the most ecologically sensitive and unique landscape type in arid and semi-arid regions. These complex and fragile geographical and ecological environments feed one-third of the world's production and support economic activities [1,2]. Oases are also natural ecological barriers against desert invasion [3] and play an important role in ecological warnings and indicators [4–7]. The oases can be regarded as the ocean on the earth [8]; they have a significant cooling effect in dry and hot seasons [9–11] and play an important role in the economic development of arid areas. Presently, owing to global warming and human activities, the desertification process in arid areas has intensified [12–15], and the ecological resources and environments of oases have also undergone significant changes [16]. Artificial oases are constantly expanding, while natural oases have shrunk [3,17]. The development of oases has also changed the spatiotemporal distribution of water resources in arid areas [18],

resulting in the deterioration of the ecological environment at the edge of oases and the expansion of deserts [3]. Dynamic changes in oasis areas have a profound impact on social and economic stability and on high-quality development in surrounding areas [1,11,19–21]. In turn, this affects the effectiveness of internal resource allocation in oases, threatening the ecological security. Therefore, there is an urgent need to strengthen the dynamic monitoring of oases in arid regions.

Under global warming, oasis environments in arid and semi-arid areas have undergone significant changes, which have drawn increased attention from the international community [3–5,22,23]. Previous studies have conducted long-term observational analysis for dynamic monitoring of oasis changes based on remote sensing (RS) and geographic information systems (GIS) [13,24,25]. Pei et al. [25] analysed dynamic changes in vegetation in Inner Mongolian grasslands from 1982 to 2015 based on the Global Inventory Monitoring and Modeling System (GIMMS) Normalised Difference Vegetation Index (NDVI) and meteorological data. Qi et al. [26] used satellite remote sensing and GIS to explore the Jinta Oasis in northwestern China. Xie et al. [27] evaluated the dynamic change of Jinta Oasis and its influence on landscape patterns in 1963–2010 based on multiple photographs and images. Liu et al. [28] identified the spatial-temporal variation characteristics of vegetation ecological systems and detected their driving forces from 1982 to 2013, based on GIMMS-NDVI and long-term meteorological station data. Some studies have used the land use transition matrix model to explore dynamic changes in vegetation; for example, Shi et al. [29] comprehensively analysed land cover change using a land-use transfer matrix and dynamic change model. Sun et al. [3] analysed the spatiotemporal variability of the oasis ecotone in the Tarim River basin using cellular automata–Markov chain (CA-Markov) methods.

Compared with the dynamic changes of oasis areas, the ecological security mechanisms play important roles in sustainable development of the oasis system. Generally, oasis ecological security has been evaluated through analysis of multiple indicators, e.g., Zhang et al. [30] evaluated the ecological environment of the arid region of Central Asia by calculating the net primary productivity (NPP) from the Carnegie–Ames–Stanford approach (CASA). Li et al. [13] evaluated the ecological environment of Central Asia through analysis of vegetation carbon sinks and sources. In addition, some studies have estimated ecological security by adopting remote sensing models; for example, Gao et al. [23] used the remote sensing ecological index (RSEI) and standard deviation ellipse algorithm to monitor the ecological quality of Hami Oasis. Hao et al. [8] analysed the influence of soil water change on near-surface temperature and the oasis effect by using the dependence framework of soil water on the evaporation rate. In terms of ecological security, Li et al. [31] evaluated the ecological security of oases in the northern Tien Shan by improving the three-dimensional ecological footprint model. However, to maintain the security and development of oases, it is necessary to comprehensively analyse the dynamic evolution of the oasis region and its driving factors, e.g., the climate, environment, and human activities. At present, most scholars analyse dynamic changes in oasis areas and the ecological security separately; studies on the dynamic change process of oases from the perspective of the whole system are lacking.

The Tarim River basin (TRB) is one of the largest basins in the world and is far away from oceans. It has a large desert in the centre and develops many oases at the border regions, which are vulnerable to climate change but important for sustaining human survival and socio-economic development. Under climate change and human disturbances, the desertification process in the TRB has intensified over the past half-century, and the desert–oasis transition zone has rapidly decreased as environmental problems have become increasingly prominent [3,18,24,28,32–35]. Current studies have indicated that the ecological environment of Xinjiang has improved with increased vegetation cover [18,28]. This is an interesting phenomenon, and it begs the question, what are the current dynamic changes of the oasis dynamics and ecological security in the Tarim River basin in the face of climate change and human activities?

Exploring the dynamic changes of the oasis and evaluating the ecological security is crucial to desertification control, oasis expansion, the security of oasis ecosystems, and ecological civilisation construction along the Silk Road Economic Belt of China. Therefore, this study investigated the spatial-temporal dynamics of oases in the TRB by exploring the spatial-temporal variation in eco-environmental quality based on several indictors of oasis (NDVI, FVC and land use) and the digital elevation model (DEM) from 2000 to 2020 and then evaluating the ecological security according to the NPP and RSEI. The main objectives of this study were to provide a theoretical basis and scientific and technological support for desert conservation, restoration, and management, as well as for sustainable economic development in arid regions.

2. Materials and Methods

2.1. Study Area

The Tarim River basin forms the largest inland basin in China. It is situated deep within the Eurasian hinterland of Northwest China and is surrounded by the Tien Shan, Karakorum, Kunlun, and Altun mountain ranges. The region is a unique enclosed inland basin that extends between 73.04° E–93.31° E and 34.84° N–43.35° N, with an area of approximately 92.60 × 10^4 km^2 (Figure 1). The TRB consists of high mountains, valley steppe, desert, and plain oasis areas and has an altitude range of 773–8323 m [36]. The Tarim River is the largest inland river in western China and is composed of 144 rivers from 9 major river systems. Currently, only the Kaidu and Aksu river in the Tien Shan (the northern TRB) and the Yarkand and Hotan rivers in the Karakoram and Kunlun mountains (the southern TRB) connect with the Tarim River (Table 1). This region includes the second largest drifting desert in the world, the Taklamakan Desert, which has an annual average temperature of 3.9 °C and annual average precipitation of 53 mm [3]. The region's water resources are relatively poor and unevenly distributed, being mainly concentrated in mountainous areas where they derive from glaciers, snow cover, and precipitation [37–40]. Precipitation is temporally and spatially uneven, with abundant precipitation in mountainous areas and rare precipitation in plain areas; precipitation mainly occurs in the summer.

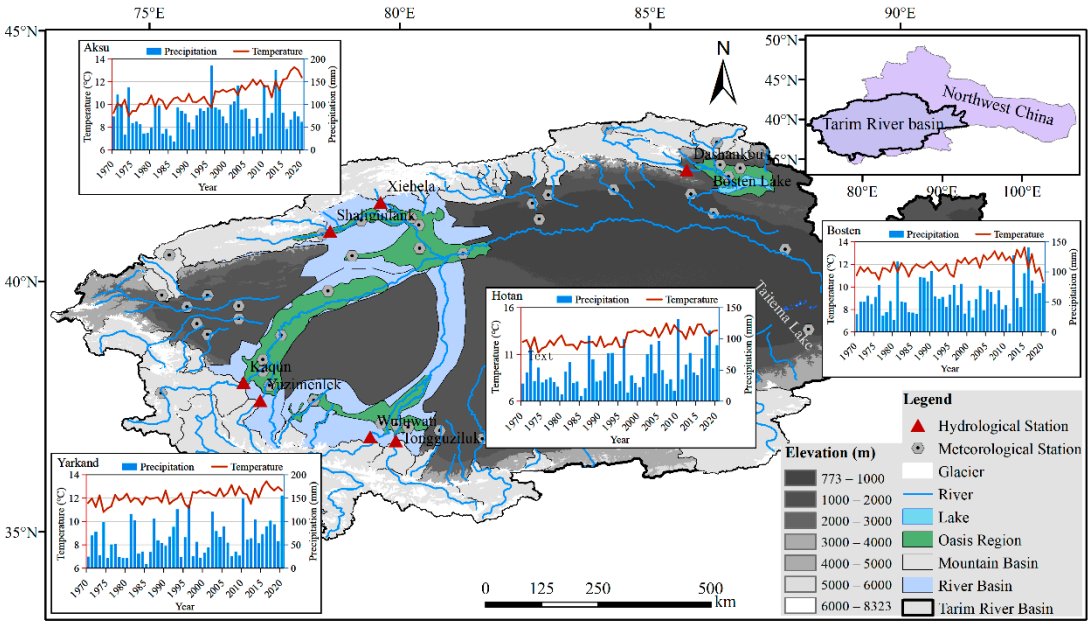

Figure 1. Map of the Tarim River basin study area. Inset plots show precipitation and temperature data along the main rivers from 1970 to 2020.

Table 1. Characteristics of the oasis information in the Tarim River basin.

Basin	Basin Area (10^4 km^2)	Oasis Region (10^4 km^2)	Fraction of Oasis Region to Basin Area (%)	Fraction of Basin Glacier Area Proportion (%)	Basin Elevation (m)	Annual Mean Runoff (10^8 km^3)
Bosten Lake	1.9	0.69	36.32	1.21	3100	11.69
Aksu River	5.0	1.56	31.20	8.92	2233	79.89
Yarkand River	3.29	1.74	52.89	11.09	4630	65.46
Hotan River	4.89	0.91	18.61	9.02	1800	23.1
Tarim River	92.6	4.90	4.80	16.34	3730	180.14

2.2. Material

To estimate the dynamic evolution of oases in the TRB and evaluate the ecological security, multiple remote sensing, climate, land use, and meteorological data from 2000 to 2020 were used in this study. The NDVI data of FVC were downloaded from MOD13Q1, with a spatial resolution of 250 m and a temporal resolution of 16 days. The NPP used in this study was estimated from the CASA model, and the NPP data from MOD17A3H, with a spatial resolution of 50 m and a temporal resolution of 8 days were used to validate the calculated NPP from the CASA model; results show that the simulated NPP from CASA consists of the NPP from MODE17A3H (R^2 = 0.83), which proved better in this study. In addition, the MOD13A1, MOD15A2H, MCD15A3H, MCD12Q1, TerraClimate, and Gladas/T3H datasets were used in this CASA model. For RSEI, the adopted datasets included MODO91, MOD11A2, and MOD13A1. The yearly land-use dataset with a spatial resolution of 1 km for the period 2000–2020 was provided by the Data Centre for Resources and Environmental Sciences, Chinese Academy of Sciences (http://www.resdc.cn accessed on 10 November 2021); this dataset has been widely used in relevant studies [3,41]. Monthly climate data between 1979 and 2020 in the TRB were obtained from the Meteorological Science Data Sharing Service N etwork (http://data.cma.cn/ accessed on 10 November 2021). The Shuttle Radar Topography Mission (SRTM1) Arc-Second digital elevation model (DEM) with a spatial resolution of 30 m was accessed via the USGS website (https://earthexplorer.usgs.gov/ accessed on 10 November 2021). All of the datasets used in this study are summarized in Table 2.

Table 2. Data product types and sources.

Product	Variable	Spatial Resolution	Temporal Resolution	Source
MOD13A1/Q1	NDVI	500/250 m	16 d	https://modis.gsfc.nasa.gov/ accessed on 10 November 2021
MOD09A1	SR	500 m	8 d	https://modis.gsfc.nasa.gov/ accessed on 10 November 2021
MOD11A2	LST	1 km	8 d	https://modis.gsfc.nasa.gov/ accessed on 10 November 2021
MOD15A2H	FPAR	500 m	8 d	https://modis.gsfc.nasa.gov/ accessed on 10 November 2021
MOD17A3H	NPP	500 m	8 d	https://modis.gsfc.nasa.gov/ accessed on 10 November 2021
MCD12Q1	Landcover (IGBP)	500 m	yearly	https://modis.gsfc.nasa.gov/ accessed on 10 November 2021
TerraClimate	SOL	4 km	monthly	https://www.ecmwf.int accessed on 10 November 2021

Table 2. *Cont.*

Product	Variable	Spatial Resolution	Temporal Resolution	Source
TerraClimate	Pre	4 km	monthly	https://www.ecmwf.int accessed on 10 November 2021
T3H(GLDAS)	Tem	0.25°	3 h	http:/ldas.gsfc.nasa.gov/ accessed on 10 November 2021
LUCC Data	Landcover	1 km	10 yearly	https://www.resdc.cn/ accessed on 10 November 2021
Meteorological Data	Tem/Pre	-	yearly	http://data.cma.cn/ accessed on 10 November 2021
SRTM	DEM	30 m	-	https://earthexplorer.usgs.gov/ accessed on 10 November 2021

Note: SR (surface reference); SOL (total solar radiation); Tem (temperature); Pre (precipitation).

2.3. Methods

2.3.1. Fraction of Vegetation Cover (FVC)

FVC is an important index to exhibit the distribution of vegetation on the ground, as well as an important parameter of ecosystem, soil erosion and climate change models. Ground measurements and remote sensing measurement are rudimental methods to observe FVC changes. Regarding the limitations of ground measurements for large regions, complex topography, and continuous observations, the estimation of vegetation by remote sensing has been widely used for FVC changes [42]. Compared with other RS methods, the FVC calculated by NDVI does not need a regression model, and it is not limited by the region or spatial, temporal and vegetation type; this approach has been widely used in the plains and mountain regions of the world, as well as arid and semi-arid regions, e.g., Central Asia [43], China [44,45] and the TRB [46–48].

FVC is closely related to NDVI and was used to quantify vegetation coverage for the TRB. In this study, we adopted the mixed-pixel dichotomy model proposed by Zeng et al. [49] to calculate the vegetation coverage. The assumption of this algorithm is that the NDVI value of each pixel consists of vegetation and soil. The specific formula is as follows:

$$NDVI = fNDVI_V + (1 - f)NDVI_S \quad (1)$$

$$f = (NDVI - NDVI_S)/(NDVI_V - NDVI_S) \quad (2)$$

where f is the FVC (%), $NDVI_V$ is the NDVI value covered by vegetation pixels and $NDVI_S$ is the NDVI value of soil or non-vegetation covered pixels. We took the maximum value of NDVI in the study area as $NDVI_V$ and the minimum value as $NDVI_S$ to calculate FVC. The FVC was divided into four grades: high vegetation coverage area (FVC $\geq$ 50%), medium vegetation coverage area (20% $\leq$ FVC < 50%), low vegetation coverage area (5% $\leq$ FVC < 20%), and bare land area (FVC < 5%).

2.3.2. NPP Estimation Using CASA

NPP represents the net primary productivity, as the rate of accumulation of biomass or energy in a unit time per unit area. It can be used as an important ecological index for quantitatively evaluating the ecological security of the terrestrial ecosystems in these arid and semi-arid areas [13,30,50]. In this study, NPP was estimated by the CASA model, realised using the Google Earth Engine (GEE). The model considers the climatic conditions (i.e., temperature, precipitation, solar radiation, NDVI and land-use data) determined by two variables: the absorbed photosynthetically active radiation (APAR) and light energy conversion (ε). This model, which was proposed by Potter et al. [51], has been widely used to estimate the NPP of regional large-scale vegetation, and it is considered to be one of the

models with the highest estimation accuracy. The detailed model, calculated as in previous studies [30,43], is as follows:

$$\mathrm{NPP}\ (x, t) = \mathrm{APAR}(x, t) \times \varepsilon(x, t) \tag{3}$$

$$\mathrm{APAR} = \mathrm{SOL} \times \mathrm{FPAR} \times 0.5 \tag{4}$$

where APAR (MJ/m^2) is the absorbed photosynthetically active radiation; FPAR is the fraction of photosynthetically active radiation, which is absorbed by green plants; ε (gC/MJ) is the light energy conversion; and SOL (MJ/m^2) is the total solar surface radiation.

$$\mathrm{FPAR_{NDVI}} = \frac{(\mathrm{NDVI} - \mathrm{NDVI_{i,min}}) \times (\mathrm{FPAR_{max}} - \mathrm{FPAR_{min}})}{\mathrm{NDVI_{i,max}} - \mathrm{NDVI_{i,min}}} + \mathrm{FPAR_{min}} \tag{5}$$

where $FPAR_{max}$ (0.95) and $FPAR_{min}$ (0.001) are independent of the vegetation type; $NDVI_{i,max}$ is the NDVI value corresponding to 95% of NDVI value; and $NDVI_{i,min}$ is the NDVI value corresponding to 5% of the NDVI value. The relationship between the FPAR and SR area is as follows:

$$\mathrm{FPAR_{SR}} = \frac{(\mathrm{SR} - \mathrm{SR_{i,min}}) \times (\mathrm{FPAR_{max}} - \mathrm{FPAR_{min}})}{\mathrm{SR_{i,max}} - \mathrm{SR_{i,min}}} + \mathrm{FPAR_{min}} \tag{6}$$

$$\mathrm{SR} = \frac{1 + \mathrm{NDVI}}{1 - \mathrm{NDVI}} \tag{7}$$

where $SR_{i,max}$ and $SR_{i,min}$ are the $NDVI_{i,max}$ and $NDVI_{i,min}$, respectively.

$$\mathrm{FAPR} = \alpha \mathrm{FPAR_{NDVI}} + (1 - \alpha)\ \mathrm{FPAR_{SR}} \tag{8}$$

with α set at 0.5. The light energy conversion (ε), given in g C/MJ, was calculated as follows:

$$\varepsilon = \mathrm{T1} \times \mathrm{T2} \times w\varepsilon \times \varepsilon\mathrm{max} \tag{9}$$

where T1 and T2 are the low- and high-temperature stresses on the efficiency of light use, respectively; wε is the effect of water stress; and εmax is the maximum light use efficiency (gC/MJ). The calculation of each stress factor and its value was based on the research results [30].

2.3.3. Dynamic Change of Oasis Areas

The dynamic change of land use type in the oasis regions was adopted to quantitatively analyse the quantity change of a certain land-use type. The equation is given as

$$\mathrm{D} = (\mathrm{U_a} - \mathrm{U_b})/(\mathrm{U_a} \times \mathrm{T}) \times 100 \tag{10}$$

where D (%) is the dynamic change of one land use in the period T (a), and U_a and U_b are the first and last years of land-use areas (km^2), respectively.

2.3.4. RSEI Estimation

With the aim of large-scale remote sensing environmental monitoring, we adopted a remote sensing monitoring indicator that reflects different ecological environmental changes and that can be retrieved from low- and medium-resolution imagery in order to calculate the RSEI for real-time and rapid monitoring of changes in eco-environmental quality. RSEI was used to evaluate the natural ecological environment of the TRB and was calculated using principal component analysis (PCA) [43]. The greenness index (NDVI), wetness index (WET), heat index (LST), and dryness index (NDSI) were used to calculate the RSEI. The formulae were as follows:

$$\mathrm{RSEI} = f(\mathrm{G}, \mathrm{W}, \mathrm{T}, \mathrm{D}) \tag{11}$$

$$\text{RSEI0} = (1 - \{\text{PC1}[f(\text{NDVI, WET, LST, NDBSI})]\}, \tag{12}$$

$$\text{RSEI} = (\text{RSEI0} - \text{RSEImin})/(\text{RSEImax} - \text{RSEImin}) \tag{13}$$

where f represents a combination of the four indicators; G, W, T, and D are the greenness index, wetness index, dryness index, and heat index, respectively; $RSEI_0$ indicates the initial value of the ecological index; PC1 represents the first component of the principal component analysis; $RSEI_{min}$ is the minimum value of $RSEI_0$; and $RSEI_{max}$ is the maximum value of $RSEI_0$. To evaluate ecological conditions, the RSEI of TRB was divided into five grades: worst (0–0.2), poor (0.2–0.4), general (0.4–0.6), good (0.6–0.8), and excellent (0.8–1).

2.3.5. Trend and Correlation Analysis

The Mann–Kendall trend test was used to identify trends in variables [52,53]; the Pearson correlation test was used to detect the degree of correlation between them; and linear regression was applied to analyse the changes in NPP, NDVI, FVC, temperature, and precipitation during 2000–2020. The Mann–Kendall test is given as

$$S = \sum_{i=1}^{n-1} \sum_{j=i+1}^{n} \operatorname{sgn}(x_j - x_i) \tag{14}$$

$$\operatorname{sgn}(x_j - x_i) = \begin{cases} 1, & x_j - x_i \\ 0, & x_j - x_i \\ -1, & x_j - x_i \end{cases} \tag{15}$$

where S is the test statistic, n is the length of the data, and x_i and x_j are the data values in the year (i) and (j), respectively.

$$\operatorname{Var}[s] = \frac{n(n-1)(2n+5) - \sum_{p-1}^{q} t_p(t_p - 1)(2t_p + 5)}{18} \tag{16}$$

where t_p and q are the number of data values and tied groups in the pth group, respectively. The test statistic (Z) was computed with Var(S) and S values, as follows:

$$Z = \begin{cases} \frac{S-1}{\sqrt{\frac{n(n-1)(2n+5)}{18}}}, & S > 0 \\ 0, & S = 0 \\ \frac{S+1}{\sqrt{\frac{n(n-1)(2n+5)}{18}}}, & S < 0 \end{cases} \tag{17}$$

The test statistic (Z) obeys the Gaussian distribution. Under the given significance level α, if $|Z| > Z_{\alpha/2}$, H0 would be rejected. If Z < 0, it means a negative trend, if Z > 0, it means a positive trend; when the absolute value of Z > 1.28, 1.64 and 2.32, it means the data pass the significant test of 90%, 95% and 99% confidence level, respectively.

The Hurst index (H) shows well in the fractal characteristics of the time series. In this study, it was used to investigate and predict the temporal-spatial dynamic changes in the oasis in the TRB. Based on the time series and the Hurst empirical formula, the Hurst index using the R/S method, which was obtained through the least-square fitting method (detailed information of this method is presented in Liu et al. [28]): (i) the variable of the oasis index is stable, the trend is constant, and the memory dynamics ($0.5 < H \leq 1$); (ii) the variable of the oasis index is random, the return is not correlated, and the series has no memory (H = 1); (iii) the series is anti-persistent, and the results are negatively correlated ($0 < H \leq 0.5$).

The procedures for evaluating of oasis ecological security are shown in Figure 2.

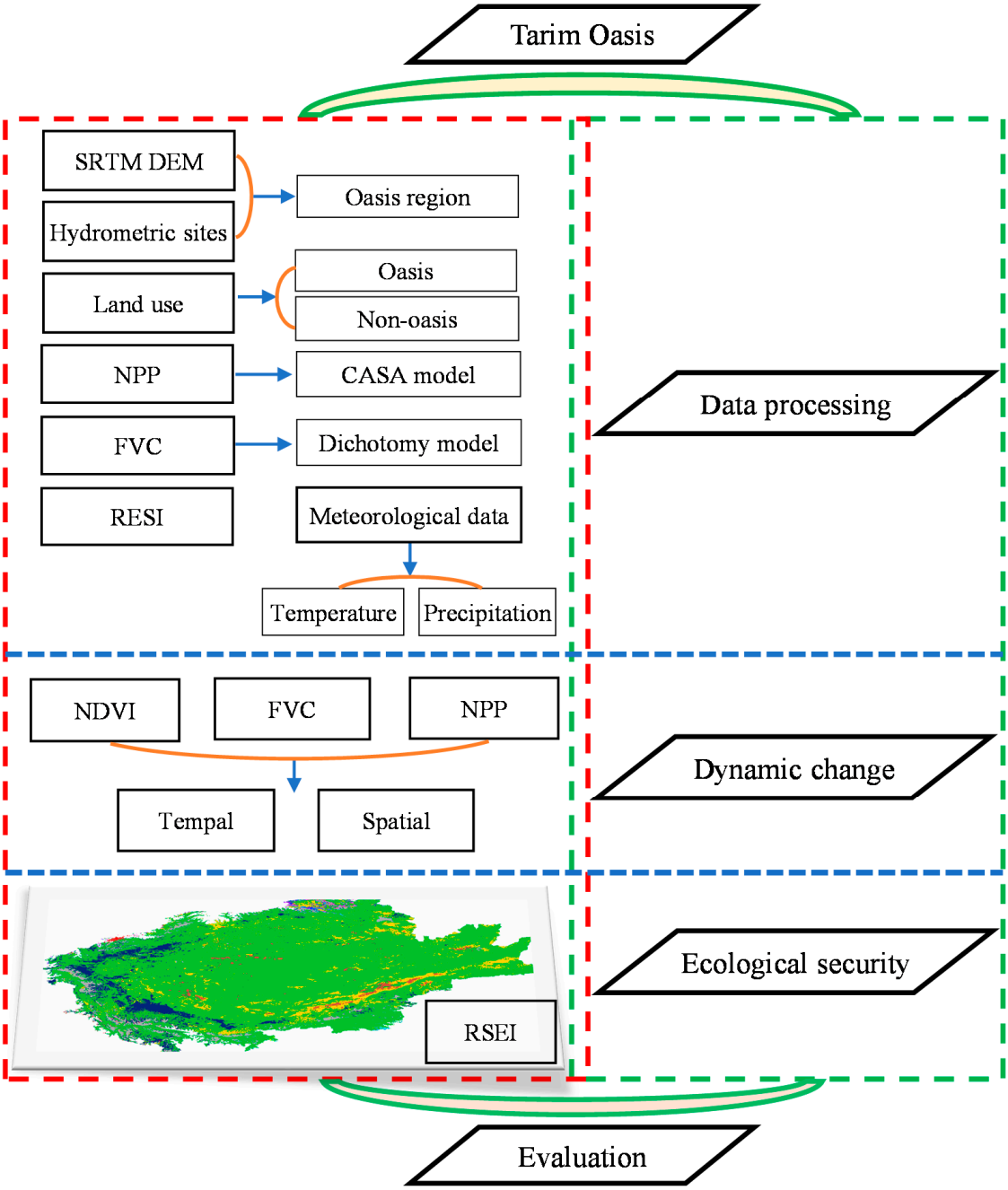

Figure 2. Flow chart showing process used for monitoring oasis dynamics and ecological security.

3. Results

3.1. Oasis Dynamic Change

Over the past 20 years, the total oasis area in the TRB showed a shrinkage trend (Figure 3), ranging from 28.43 × 10^4 km^2 in 2000 to 28.15 × 10^4 km^2 in 2020 (i.e., a total area decrease of 0.18 × 10^4 km^2 or 0.65%). However, the individual plain oases showed notable expansion, with area expanded by 8.21% during the study period. This is particularly the case for the Aksu River basin (ARB) and Bosten Lake basin (BLB), in which the areas expanded by 1268 km^2 (11.64%) and 335 km^2 (10.48%), respectively, during 2000–2020. Oasis areas in the Yarkand River basin (YRB) and Hotan River basin (HRB) increased by 974 km^2 (7.5%) and 122 km^2 (2.1%), respectively. However, it is worth noting that the oasis area in the HRB decreased by 75 km^2 (1.25%) from 2015 to 2020.

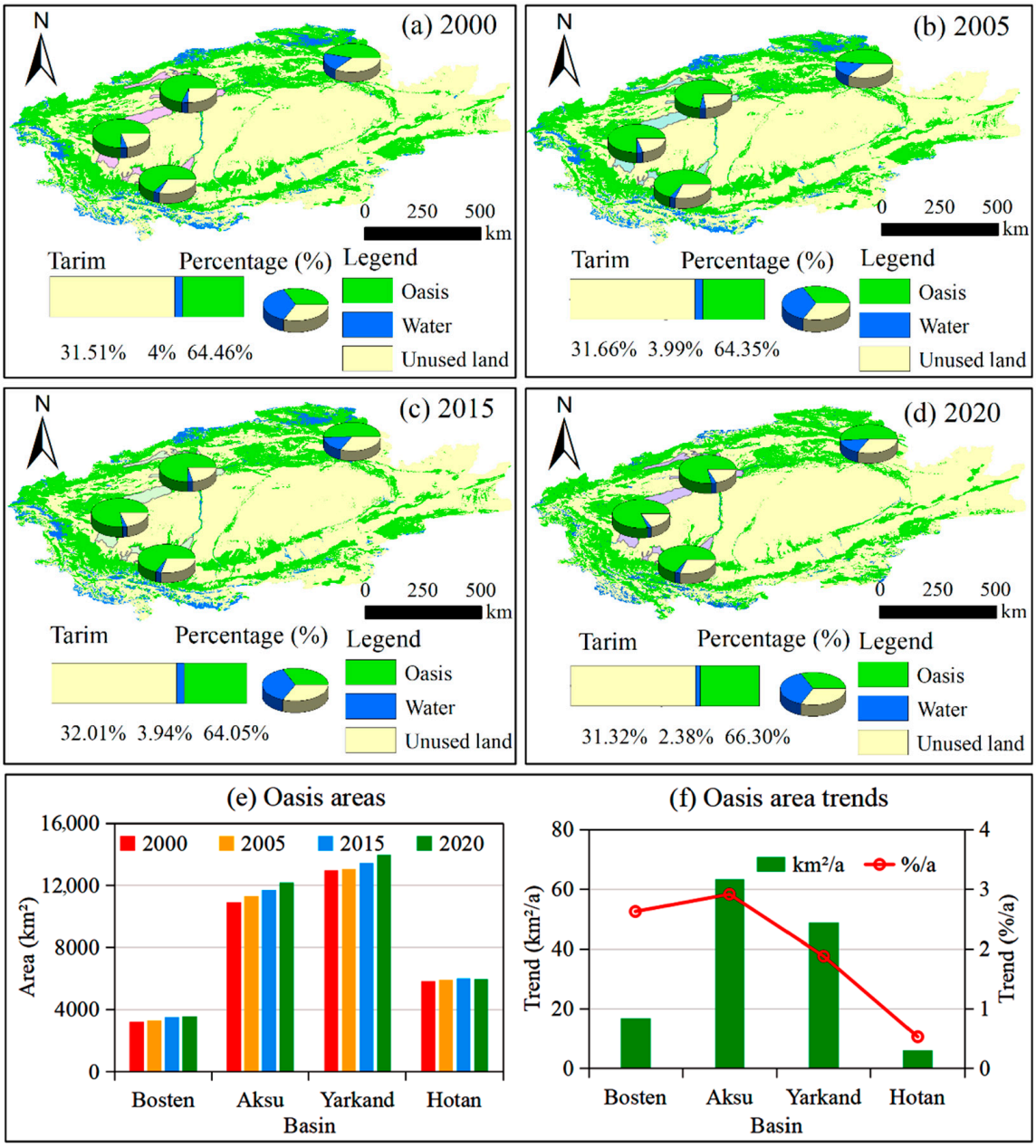

Figure 3. Variation in oasis area in the Tarim River basin (TRB) during 2000–2020. Oasis area in (**a**) 2000, (**b**) 2005, (**c**) 2010, and (**d**) 2020. (**e**) Temporal evolution of oasis area and (**f**) change rates in oasis area.

3.2. Indictors of Oasis Change

3.2.1. NDVI

Based on the changes in NDVI in the TRB oases from 2000 to 2020, the NDVI value showed a significant increasing trend over the past 20 years ($p < 0.01$), with NDVI increasing from 0.13 in 2000 to 0.16 in 2020, with an increase rate of 27.06%. Spatially, 90.06% of the TRB NDVI values showed a positive trend, while only 9.94% exhibited a negative trend. In the subbasins of the TRB, all basins showed positive trends; for example, the NDVI in the YRB and HRB increased by 0.10 and 0.08, with expansion rates of 30.38% and 32.51%, respectively. For the BLB and ARB, the NDVI value increased by 0.11 and 0.18, with rates increased by 38.41% and 51.61%, respectively (Figure 4f).

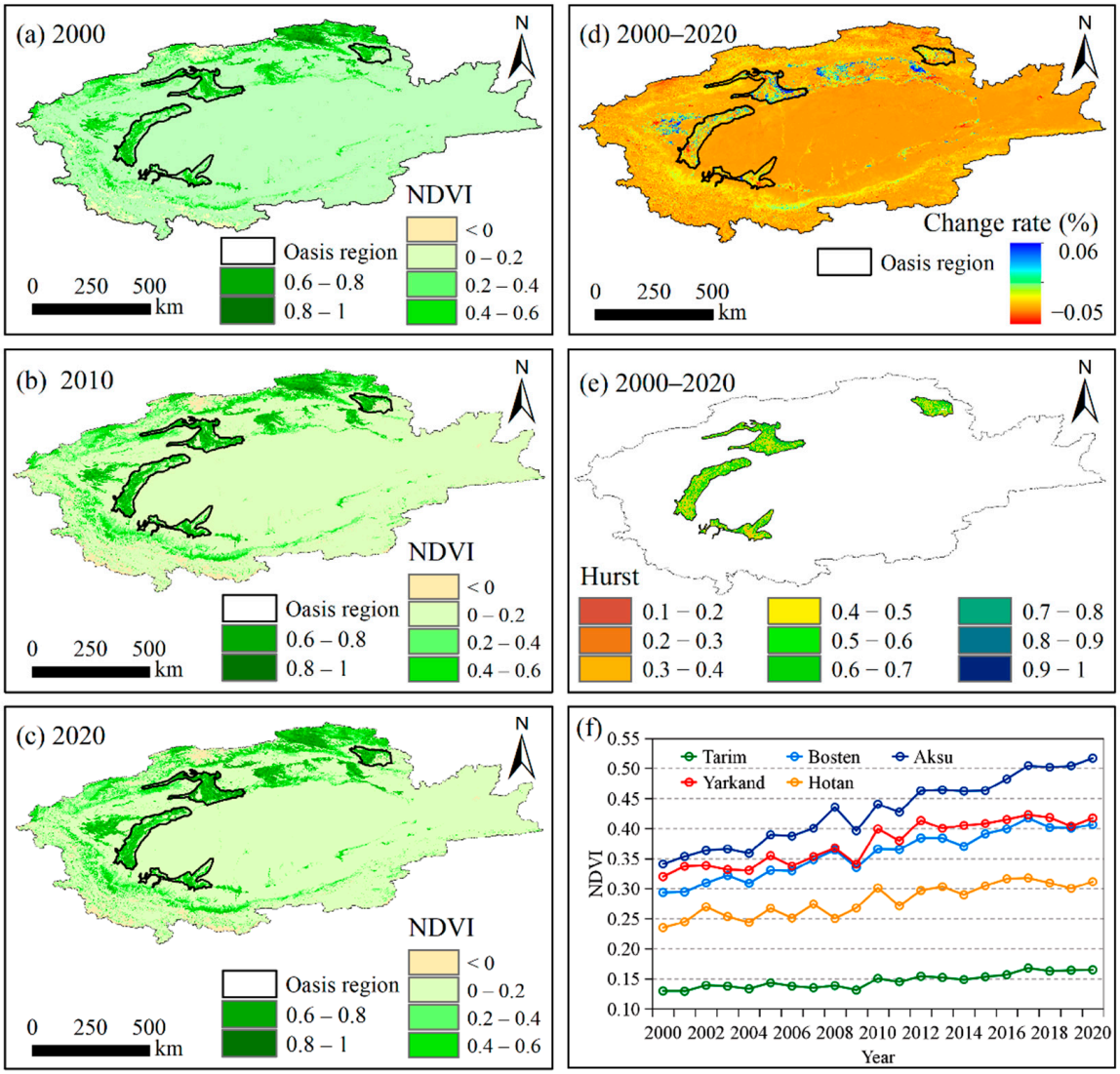

Figure 4. Variation in the Normalised Difference Vegetation Index (NDVI) of the Tarim River basin (TRB) during 2000–2020: NDVI in (**a**) 2000, (**b**) 2010, and (**c**) 2020. (**d**) Spatial variation trend of NDVI, (**e**) temporal evolution of the Hurst index, and (**f**) temporal evolution of NDVI in the basins.

During different periods, NDVI showed different rates in different basins (Figure 4a–c). During 2000–2010, the NDVI value in the TRB increased by 0.02 (27.06%), and the NDVI in the HRB, YRB, BLB, and ARB oases increased by 28.03%, 24.74%, 24.60%, and 29.16%, respectively. After 2010, the increase rate of NDVI in the TRB slowed. For example, the increased rates of NDVI in the BLB and ARB were 11.09% and 17.38%, respectively, which was half of the increased NDVI during 2000–2010. The increase rates of NDVI in the YRB and HRB oases during 2000–2020 were significantly lower than that during 2000–2010, with increase rates of 4.52% and 3.50%, respectively.

The spatial distribution of the Hurst index (Figure 4e) indicates that the ecological environment of most regions of the TRB will be degraded in the future; ~60% of the BLB, ARB, and YRB NDVI values have decreased, while 91.15% of the NDVI values are continuing to deteriorate. It is worth noting that 8.85% of the regions of the TRB saw an improvement in NDVI, with most of these areas concentrated in and around river channels.

3.2.2. FVC

According to the spatial distribution and variation trend of FVC in the TRB from 2000 to 2020 (Figure 5), the average annual FVC in the TRB was less than 30%. The average

annual FVC in the BLB and ARB oases (in the Tien Shan of the northern TRB) were 37.64% and 46%, respectively. The average annual FVC of the YRB plain oasis (in the Karakorum and Kunlun mountain ranges of the southern TRB) was 42.91%, while that of the HRB oasis was only 30.55%. The annual FVC of the TRB basins increased significantly ($p < 0.01$) over the 20 year interval, with an increase rate of 0.27%/a. From 2000 to 2020, the FVC of the TRB oasis increased significantly ($p < 0.01$), and the FVC of the HRB, YRB, BLB, and ARB oases increased by 0.21%/a, 0.54%/a, 0.66%/a, and 0.85%/a, respectively.

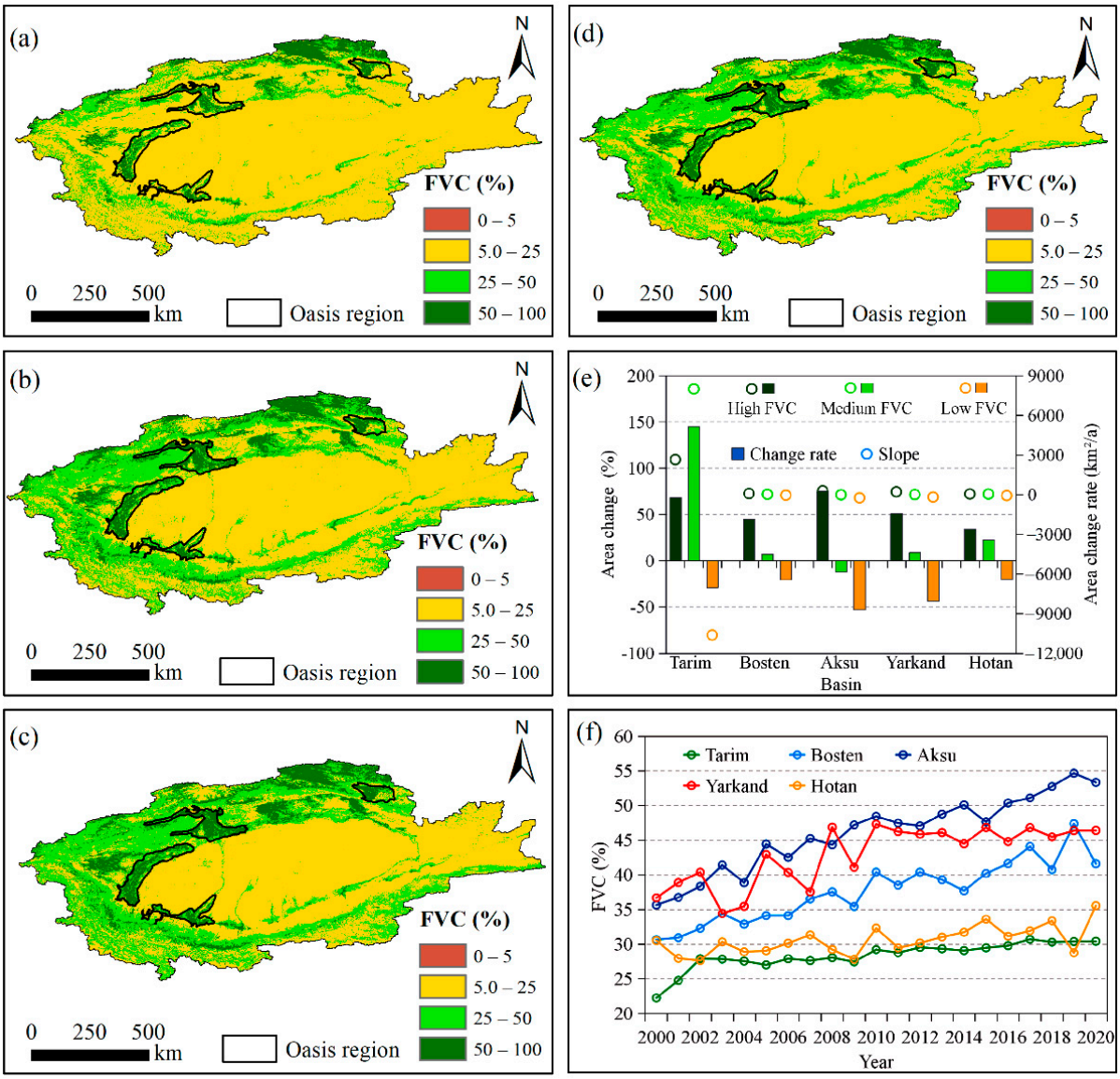

Figure 5. Spatial variation in the fraction of vegetation cover (FVC) in the Tarim River basin (TRB) oasis during 2000–2020. FVC in (**a**) 2000, (**b**) 2010, and (**c**) 2020. (**d**) Spatial distribution of average FVC, (**e**) change rates in FV, and (**f**) temporal evolution of FVC.

High and medium FVC areas in the TRB (Table 3) showed obviously positive trends ($p < 0.01$), with areas expanded by 37.99% and 145.07%, respectively; however, the proportion and area of the low FVC area showed obvious negative trends ($p < 0.01$), with the proportion increasing by 31.77% and the area decreasing by 29.17%. Spatially, the high and medium FVC areas (except the medium FVC in the ARB and YRB) exhibited notable expansion trends ($p < 0.05$), with areas expanding by 44.79% and 6.99% in the BLB, 74.82% in the ARB, 52.96% in the YRB, and 33.89% and 22.53% in the HRB. In contrast, the low FVC areas in the BRB, ARB, YRB, and HRB showed significant negative trends ($p < 0.01$),

with areas decreasing by 20.51%, 52.74%, 45.50%, and 20.20%, respectively. Meanwhile, the medium FVC in the ARB showed an obvious negative trend ($p < 0.05$), with the area decreasing by 12.10%.

Table 3. Fraction of vegetation cover (FVC) variation in the Tarim River basin (TRB) oases.

Basin	Variables	High FVC	Medium FVC	Low FVC
BLB	Average (%)	69.17	37.19	13.37
	Change (%)	9.23	−4.09	11.52
	Z value (FVC)	3.96 (**)	−3.71 (**)	3.93 (**)
	Area change (%)	44.79	6.99	−20.51
	Z value (Area)	5.41 (**)	2.39 (*)	−4.80 (**)
ARB	Average (%)	68.40	37.01	15.66
	Change (%)	10.32	−2.32	28.26
	Z value (FVC)	3.65 (**)	−1.51	1.36
	Area change (%)	74.82	−12.10	−52.74
	Z value (Area)	6.01 (**)	−2.26 (*)	−5.59 (**)
YRB	Average (%)	68.44	36.11	16.46
	Change (%)	10.32	−2.32	28.26
	Z value (FVC)	0.51	1.90	1.54
	Area change (%)	52.96	9.55	−45.50
	Z value (Area)	5.10 (**)	−0.09	−3.84 (**)
HRB	Average (%)	66.75	36.45	11.79
	Change (%)	0.80	2.16	−8.22
	Z value (FVC)	−1.78	2.66 (**)	0.82
	Area change (%)	33.89	22.53	−20.20
	Z value (Area)	3.77 (**)	3.96 (**)	−3.23 (**)
TRB	Average (%)	65.63	32.43	21.37
	FVC Change (%)	3.48	−5.39	31.77
	Z value (FVC)	4.50 (**)	−0.91	5.16 (**)
	Area change (%)	67.99	145.07	−29.17
	Z value (Area)	4.50 (**)	4.80 (**)	−4.86 (**)

Symbols: *. Significance $p < 0.05$; **. Significance $p < 0.01$.

3.2.3. NPP

From 2000 to 2020, the NPP in the TRB increased significantly ($p < 0.01$), with an increase of 31.55% at a rate of 0.50 g C/m^2·a. Spatially, the average annual NPP in the BRB and ARB oases was 101.30 and 112.09 g C/m^2, respectively, which is higher than the southern basins of the TRB (the HRB oasis with an average annual NPP of 72.04 g C/m^2 and the YYRB oasis with average annual NPP of 95.57 g C/m^2). The NPP of the four basin oases in the TRB showed a significant increasing trend ($p < 0.01$) during the study period. The NPP of the BRB, ARB, YRB, and HRB oases increased by 2.26, 2.86, 2.03, and 1.39 g C/m^2, respectively, with expansion rates of 98.51%, 56.13%, 66.42%, and 49.56%, respectively.

The Hurst index (H) of the NPP in the TRB from 2000 to 2020 was 0.47, indicating that the positive trend in NPP will be inverse in the future; however, there were obvious spatial differences (Figure 6f). For the Hurst value in the sub-basins of the TRB, the NPP in the YRB and HRB oases is predicted to decrease, particularly in the HRB (H = 0.27); in contrast, the NPP in the BLB (H = 0.57) and ARB (H = 0.53) oases will increase in the future. Figure 6e shows the spatial distribution of H in the TRB, which indicates that more than half of the regions' NPP in the BRB, ARB, and YRB oases will still show positive trends in the future; the proportion of the increased NPP in the ARB oasis is 64.52%. For the future trend of NPP in the HRB oasis, more than half (51.25%) of the region will show a negative trend, while 48.75% of the region will exhibit a positive trend.

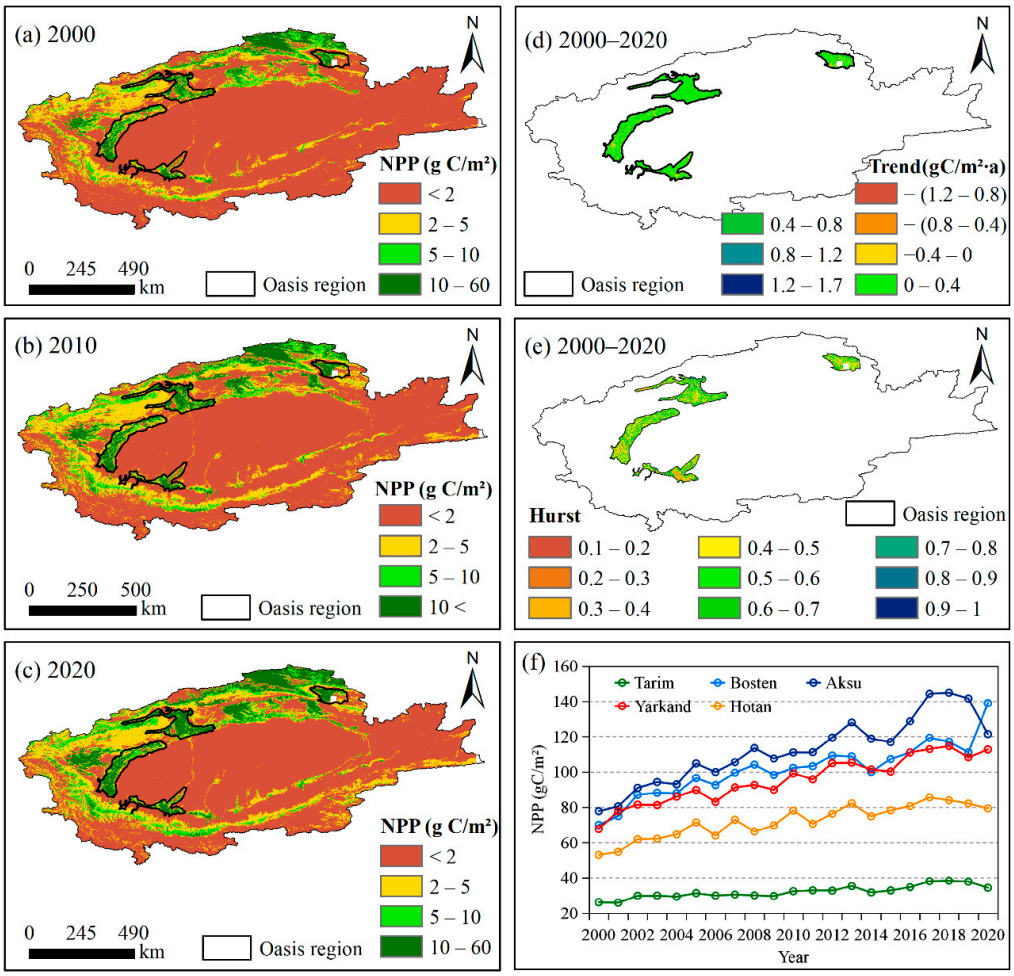

Figure 6. Spatial variation in the net primary productivity (NPP) of the Tarim River basin (TRB) oases during 2000–2020. NPP in (**a**) 2000, (**b**) 2010, and (**c**) 2020. Variation trends of (**d**) NPP and (**e**) its Hurst index in the sub-basins of the TRB, and the (**f**) temporal evolution of NPP in the TRB.

3.3. Evaluation of Ecological Environment

The RSEI of the TRB (Table 4) increased from 0.28 in 2000 to 0.43 in 2020, an increase of 52.31%. Spatially, most ecological environments of the TRB range from the worst grade to the poor grade; mountain regions ranged from poor to medium-good grade. During 2000–2020, the RSEI increased from 0.33 to 0.45 in the BLB, and from 0.39 to 0.55 in the ARB, increases of 35.63% and 42.53%, respectively. For the southern TRB, the RSEI increased from 0.41 to 0.45 in the YRB, and from 0.29 to 0.42 in the HRB, representing increases of 10.81% and 45.02%, respectively.

Compared with 2000, the total area of the worst and poor grades in the TRB decreased by 86.87% and 22.96%, respectively. The good and excellent grade regions increased by 140.02%. From 2000 to 2020, the significantly degraded region and the relatively degraded region accounted for 5% of the TRB. The stable region accounted for 26.08%, and the relatively improved region accounted for 62.69%, whereas the significantly improved region accounted for 6.23%. In terms of spatial changes, most regions were stable; the relatively improved region and the relatively degraded region were less than 7%, and the significantly degraded region was less than 2%.

Overall, the ecological environment of the TRB has improved in recent years, especially in the western mountainous area (e.g., the HRB, YRB, and ARB oases). However, in the western and southwestern TRB, the ecological environment has degraded (e.g., the Kongi River basin and Cherchen River basin; Figure 7).

Table 4. Remote sensing ecological index (RSEI) and area proportions of different ranking regions in the Tarim River basin (TRB) and its oases from 2000 to 2020.

Region	RSEI	TRB	BRB	ARB	YRB	HRB
				%		
Significant degraded region	<−0.2	1.24	0.1	1.69	0.01	0.07
Relatively degraded region	−0.2~−0.05	3.77	6.02	3.20	0.73	6.66
Stable region	−0.05~0.05	26.08	57.63	43.92	23.20	35.57
Relatively improved region	0.05~0.2	62.69	34.24	49.71	74.34	48.50
Significantly improved region	>0.2	6.23	2.01	1.48	1.72	9.21

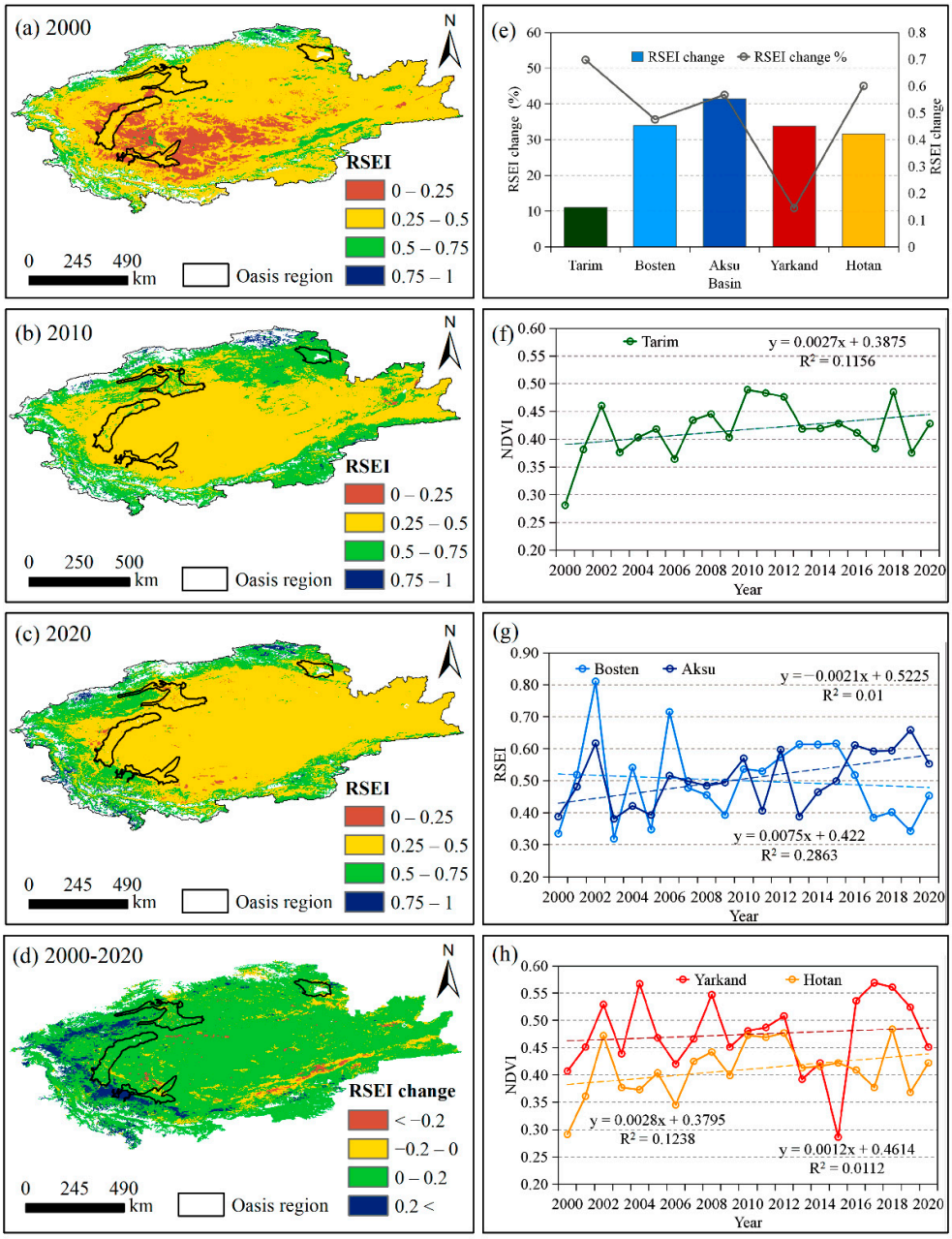

Figure 7. Spatial variation in the remote sensing ecological index (RSEI) of Tarim River basin (TRB) oases during 2000–2020. RSEI in (**a**) 2000, (**b**) 2010, (**c**) 2020; (**d**) spatial variation in RESI; (**e**) variation in RSEI in the TRB; (**f**) temporal evolution of RSEI in the TRB; (**g**) temporal evolution of RSEI in the BLB and ARB; (**h**) temporal evolution of RSEI in the YRB and HRB.

4. Discussion

4.1. Climatic Influences

Over the past half-century, both temperature and precipitation in the TRB have increased (Figure 1). From 1970 to 2020, temperature and precipitation increased by 0.37 °C/10a and 6.09 mm/10a, respectively, which is consistent with Central Asia [54] but higher than that of the Tien Shan region (0.32 °C/10a and 5.82 mm/10a) [55]. The rapid temperature increase may be the main reason for vegetation degradation and desert expansion in the desert–oasis transition zone in the TRB in recent decades. It is notable that the temperature in the TRB increased slowly, by 0.2 °C/10a, between 2000 and 2020, while the increased precipitation reached 16.43 mm/10a. Liu et al. [56] revealed that the Xinjiang region has experienced a so-called 'warm and wet transition' since the late 1980s. The current slower warming climate, with a positive trend in precipitation, may have contributed to the improved ecological environment, including the increased NDVI and NPP and expanded FVC. Previous studies have confirmed the results; e.g., Wang et al. [18] found the vegetation vigour and coverage have increased. Liu et al. [28] detected that, in Xinjiang, the warmer and wetter conditions have contributed to the expansion of vegetation cover. Xu et al. [57] observed that both the grassland and cropland in southern Xinjiang showed a significant expansion trend over the past decades. Song and Zhang [58] indicated that climate changes in temperature and precipitation had positive influences on oasis expansion (43.65%) from 1986 to 2011.

A water resource is the essential factor for the development of oases, and it is the most direct factor restricting economic development and ecosystems in arid areas. Except for the warming and wetting of the climate, the increasing river runoff recharge by glacier and snow meltwater in the upper reaches is also an important reason for the expansion of oasis areas in the lower reaches of the Tarim River. In recent decades, the runoff of the Tarim River showed an obvious positive trend [59–61], e.g., for the Aksu River, which is the largest replenishment source of the Tarim River, the runoff increased by 30% from 1957 to 2004 [62], and the runoff of its two major tributaries (the Kumalak River and Toxkan River) also showed positive trends of 0.56×10^8 and 1.83×10^8 m^3/10a from 1979 to 2015, respectively [38]. From 1972 to 2016, the annual runoff of the Kaidu River increased by about 226 million m^3/10a [63], and the runoff of the Hotan River showed a higher increase after 1990, which was mainly controlled by summer runoff [64]. The annual increasing rate of runoff in the Yarkand River reached 0.5%/a from 1968 to 2017 [65]. Ye et al. [66] found that 71% of lake levels in Xinjiang presented a positive trend from 2003 to 2009, especially the lakes in the TS region. Similarly, the expansion rate of lake areas (0.98%/a) during 2000–2013 was approximately four times the rate (0.23%/a) from 1990 to 2000 [67]. Overall, both the warm and humid climate and increased meltwater from glacier and snow contributed to the oasis expansion. Compared with the aggravated arid zone resulting in the significant expansion of the carbon source area in Central Asia from 2001 to 2008 [30], the improved ecological environment of the TRB will help to reduce the carbon source, and some regions may turn into carbon sink areas. In the United States, the carbon sink of grasslands is affected by drought and is in a poor state; however, some regions have changed to carbon sources [68].

4.2. Human Activities

Human disturbance caused by population growth, social and economic development, and highly intensive utilization of resources is becoming a global problem that results in a degrading ecosystem and influences the ecological environment in arid regions. The ecological environment in arid areas is fragile, and it is especially sensitive and vulnerable to human disturbance. In addition, the drying effects of climate change also indicate that ecological problems caused by drought events will increase in the future [69–71]. Oases are regarded as the most important regional systems of man–land relationships in arid areas; they serve as the active area in the diffusion of production and living in arid areas. The increase in oases disturbed by human activities has brought great challenges to the

coordination of water resource allocation. The distribution of oases in arid areas depends on river runoff, which provides a wide range of ecosystem services and water resources [72]. Wang et al. [29] found that the influence of human activities on the ecological environment in the Aral Sea basin of Central Asia was greater than the impact of climate change, based on the RSEI method. Chen et al. [1] found that human activities are the dominant driving force governing the expansion or shrinkage of oasis areas in the Shiyang River basin, with mean contributions of 69.38% and 76.16%, respectively, and that policy decisions are the pivotal human factor. Despite this, the Jinta Oasis of the Heihe River basin grew during 1963–2010, as a result of the wasteland area being converted into cultivated land, constructive land and forestland [27]. With the influence of human activities in recent years, the vegetation ecosystem in the Tarim River basin has been seriously degraded. For example, the NDVI in the Desert-Oasis Ecotone of the Tarim River basin decreased by 0.015 from 1990 to 2015 [71]. According to statistics, land cover area of the desert–oasis ecotone region in Xinjiang decreased by 43%, while the oasis area expanded by nearly 35% during 1990–2008 [73]. From 1990 to 2008, the artificial oases in the Aksu River basin increased significantly, with shifts in policy, enhancement of human activities, and changes in climate and runoff being the main driving forces [74]. The protection and restoration of natural and artificial vegetation in oases is the key to maintain the sustainable development of arid and semi-arid regions. Since 2000, to protect and restore the dominant natural species of desert riparian forests, the government of China began to implement the "Ecological water diversion Project, EWCP" [75]. Ling et al. [76] evaluated the positive impact of EWCP on the growth of desert vegetation in the arid basin. Ye et al. [14] found that the area of Taitema Lake expanded by 144% from EWCP, which greatly improved the ecology of the area and the water quality of the lake [14].

Between 2000 and 2020, the mutual transformation of different land use/cover types in the TRB was severe (Table 5), especially for cultivated and urban construction land; cultivated land area in the TRB increased by 15,324 km^2 (56.95%), while forest and grassland areas decreased by 1150 km^2 (8.36%) and 17,639 km^2 (7.28%), respectively. In terms of the dynamic changes of land types in the TRB, the cultivated land area expanded significantly from 2000 to 2020, accompanied by a significant decrease in forest and grassland areas. During the study period, the cultivated land areas in the BLB, ARB, YRB, and HRB oases expanded by 633 km^2 (35.24%), 2852 km^2 (50.68%), 1903 km^2 (34.26%), and 1011 km^2 (53.10%), respectively. However, the forest and grassland areas in the TRB decreased significantly during the same period. The forest areas of the BLB, ARB, YRB, and HRB decreased by 171 km^2 (90.48%), 631 km^2 (55.94%), 500 km^2 (43.67%), and 161 km^2 (57.50%), respectively. The total grassland area in these basins decreased by 217 km^2 (19.60%), 1198 km^2 (30.65%), 638 km^2 (10.55%), and 721 km^2 (20.77%), respectively.

Table 5. Land use types and area changes in the Tarim River basin (TRB) during 2000–2020.

	Year	Basin	Oasis				Non-Oasis	
			Cultivated Land	Forest	Grassland	Industrial Land	Water	Unused Land
Area change	Km^2	TRB	15,324	−1150	−17,639	−14,629	1620	16,902
	%		56.95	−8.36	−7.28	−40.55	112.73	2.91
	Km^2	BLB	633.00	−171.00	−217.00	−61.00	90.00	−274.00
	%		35.24	−90.48	−19.60	−5.46	86.54	−10.59
	Km^2	ARB	2852.00	−631.00	−1198.00	−130.00	245.00	−1138.00
	%		50.68	−55.94	−30.65	−17.36	107.46	−28.55
	Km^2	YRB	1903.00	−500.00	−638.00	−421.00	209.00	−553.00
	%		34.26	−43.67	−10.55	−45.96	87.82	−15.71
	Km^2	HRB	1011.00	−161.00	−721.00	−31.00	−7.00	−91.00
	%		53.10	−57.50	−20.77	−7.81	−4.19	−3.20

Over the same period, the water area in the TRB increased by 1620 km^2 (112.73%), while the unused land area (main desert and bare land) increased by 2.91%. In addition, the water bodies of all basins expanded, except for the HRB, which had an area decrease of 7 km^2 (4.19%). However, unused land in the TRB decreased from 2000–2020, with areas

decreased by 274 km^2 (4.19%) in the BRB, 1138 km^2 (28.55%) in the ARB, and 209 km^2 (7.82%) in the YRB.

Overall, the cultivated land in the TRB expanded significantly between 2000 and 2020, which severely squeezed forest and grassland areas and amplified the utilisation of land use in non-oasis areas; urban construction land expanded by 112.73%. Meanwhile, the used land area expanded by 2.91%, whereas the unused land area decreased significantly; for example, these areas in the BLB and YRB oases decreased by 10.59% and 15.71%, respectively, and those in the ARB decreased by 28.55%. This further indicates that human activities have a great impact on land use in the TRB, including the expansion of bare land and the reduction in grassland area in the oasis–desert zone.

In recent decades, the population and agricultural areas of the TRB have increased rapidly. According to the 2016 Xinjiang Statistical Yearbook, the basin has a population of more than 11 million and an agricultural area of 2819×10^3 ha, with more than one-third of the area facing water resource shortages (World Resources Institute's Aqueduct Global Water Risk Map, http://www.wri.org/our-work/project/aqueduct accessed on 10 November 2021). The increased population, the need for economic development, and the process of urbanisation have all intensified the pressure on regional natural resources and the environment. With the gradual expansion of cultivated land area in oases, the ecological space of the desert–oasis transition zone is strongly occupied, and this has caused a continuous decrease in the desert–oasis transition zone area [3]. Despite the oasis areas showing positive trends under human activities, water demand has increased for surface and groundwater. For example, during the expansion of the Heihe Oasis area from 2000 to 2010, the agricultural land expanded by 11%, while the total irrigation water demand increased by 6.3% [2]. Fu et al. [77] revealed that human effects significantly changed the distribution and allocation of limited water resources in the basin, leading to the oasis expansion. Deng and Chen [78] found that human activities were the main reason for the decrease in terrestrial water storage in the northern TRB. Therefore, strengthening and reasonably controlling water resources in the TRB is an important measure to prevent further deterioration of the ecological environment and to realise sustainable and healthy development.

5. Conclusions

This study investigated dynamic changes in oases and evaluated ecological security across the TRB during the period 2000–2020. Our main conclusions are as follows:

The total oasis area in the TRB decreased by 0.65%, but the plain oasis area increased significantly (8.21%) from 2000 to 2020. Specifically, the artificial oases (cultivated and industrial land) showed a notable increase (53.36% and 19.09%), whereas the natural oases (forests and grassland) exhibited an apparent decrease (43% and 72.86%). Spatially, the total oasis areas in the northern TRB (e.g., ARB and BLB) showed higher expansion area in comparison to the southern TRB (YRB and HRB).

The indictors of oasis change in the TRB were greatly improved over the past 20 years. The NDVI of the TRB oases increased from 0.13 in 2000 to 0.16 in 2020. In addition, the FVC increased significantly (36.79%), and the NPP increased by 31.55%. Spatially, the NDVI, FVC, and NPP increased by 24.60%, 35.76%, and 98.51%, respectively, in the BLB oasis; 29.16%, 49.70%, and 56.13% in the ARB oasis; 24.74%, 26.53%, and 66.42% in the YRB oasis; and 28.03%, 16.49%, and 49.56% in the HRB oasis.

From 2000 to 2020, the entire ecological environment of the TRB improved, with the ecological grade changing from a poor grade (0.28) to a general grade (0.43). Approximately 69% of the TRB's eco-environment experienced a relative improvement, mainly distributed in the western mountains. The degraded ecological environment area was less than 5%, mainly occurring in the desert–oasis ecotone. Spatially, the ecological restoration areas of the BRB, ARB, and HRB were 36.25%, 51.19%, and 57.71%, respectively. The ecological restoration area of the YRB was 76.06%, and the ecological degradation area of each basin was less than 7%.

With a continuously changing climate and human disturbances, the oases in the TRB have experienced great change. The recent ecological environment of the TRB is improving, as plain oases are expanding significantly. Population increase promotes the transformation of other land types to arable land and industrial land and translates natural oases and non-oases to artificial oases. Despite the total oasis areas have been greatly expanded, the natural oasis areas presented a shrinking trend, especially for the natural oases in the desert–oasis ecotone, which will become more vulnerable. Owing to the rapid expansion of the cultivated land, there has been a strong shrinkage of ecological water use and an acceleration of expanded moderate and light desertification on oasis peripheries. The ecological environment of the oasis is more fragile, and water problems in these regions have become more prominent. The internal analysis of the dynamic changes in oasis shows that human activities are an important reason for the fragmentation of the oases' ecological landscape. There is an urgent need to strengthen the coordinated management of oasis ecological security in arid regions.

This work studied the dynamic changes of the oasis, evaluated the ecological security in the TRB, and detected the driving factors affecting the oasis change, including land use, oasis indictors, climate, and human activities. However, the change of the oases in the arid region is a long-term and complex issue, which is affected by climate change, human activities, topography, policies, and other aspects. Further research is needed to more scientifically and accurately analyse the oasis changes and ecological security in the TRB, e.g., the water resource changes, which are mainly influenced by mountain melt water from glacier and snow, the ground water level changes, the allocation and utilization of water resources, and the development of farm land. Thus, combining information from glaciers, snow, and meteorological and hydrological data by using the glacial-hydrological model, the future land use planning by the government and the total water storage in terms of the future development of oases will be the aim of future research.

Author Contributions: Q.Z. and C.S. conceived of the original design of the paper, contributed to the manuscript writing and reviewing; Y.C. contributed to conceptualization; Y.X. contributed to data processing and formal analysis; W.C., J.L. and Y.L. provided comments on this paper. All authors have read and agreed to the published version of the manuscript.

Funding: The research is supported by International Cooperation program of Chinese Academy of Sciences (131965KYSB20210045) and the National Natural Science Foundation of China (52161145102).

Institutional Review Board Statement: Not applicable.

Informed Consent Statement: Not applicable.

Data Availability Statement: MODIS datasets of MOD13A1/Q1, MOD09A1, MOD11A2, MOD15A2H, MOD17A3H and MCD12Q1 can be found at https://modis.gsfc.nasa.gov/ (accessed on 10 November 2021); TerraClimate datasets were obtained from https://www.ecmwf.int (accessed on 10 November 2021); GLDAS data were obtained from http:/ldas.gsfc.nasa.gov/ (http://data.cma.cn/ (accessed on 10 November 2021); LUCC Data were obtained from https://www.resdc.cn/ (accessed on 10 November 2021); Meteorological data were provided by http://data.cma.cn/ (accessed on 10 November 2021); SRTM DEM data were obtained from https://earthexplorer.usgs.gov/ (accessed on 10 November 2021).

Conflicts of Interest: The authors declare no conflict of interest.

References

1. Chen, Y.; Yang, G.; Zhou, L.; Liao, J.; Wei, X. Quantitative Analysis of Natural and Human Factors of Oasis Change in the Tail of Shiyang River over the Past 60 Years. *Acta Geol. Sin.* **2020**, *94*, 637–645. [CrossRef]
2. Zhou, D.; Wang, X.; Shi, M. Human Driving Forces of Oasis Expansion in Northwestern China During the Last Decade—A Case Study of the Heihe River Basin. *Land Degrad. Dev.* **2016**, *28*, 412–420. [CrossRef]
3. Sun, F.; Wang, Y.; Chen, Y.; Li, Y.; Zhang, Q.; Qin, J.; Kayumba, P.M. Historic and Simulated Desert-Oasis Ecotone Changes in the Arid Tarim River Basin, China. *Remote Sens.* **2021**, *13*, 647. [CrossRef]
4. Huang, J.; Ji, F. Effects of climate change on phenological trends and seed cotton yields in oasis of arid regions. *Int. J. Biometeorol.* **2015**, *59*, 877–888. [CrossRef]

5. Cao, G.L.; Zheng, C.M.; Simmons, C.T. Groundwater recharge and mixing in arid and semiarid regions: Heihe River Basin, Northwest China. *Acta Geol. Sin.* **2016**, *3*, 971–987. (In Chinese)
6. Zhou, X.; Lei, W. Hydrological interactions between oases and water vapor transportation in the Tarim Basin, northwestern China. *Sci. Rep.* **2018**, *8*, 13431. [CrossRef] [PubMed]
7. Zuo, L.; Zhang, Z.; Zhao, X.; Wang, X.; Wu, W.; Yi, L.; Liu, F. Multitemporal analysis of cropland transition in a climate-sensitive area: A case study of the arid and semiarid region of northwest China. *Reg. Environ. Chang.* **2014**, *14*, 75–89. [CrossRef]
8. Feistel, R.; Hellmuth, O. Relative Humidity: A Control Valve of the Steam Engine Climate. *J. Hum. Earth Future* **2021**, *2*. [CrossRef]
9. Hao, X.; Hao, H.; Zhang, J. Soil moisture influenced the variability of air temperature and oasis effect in a large inland basin of an arid region. *Hydrol. Process.* **2021**, *35*, e14246. [CrossRef]
10. Liu, R.; Sogachev, A.; Yang, X.; Liu, S.; Xu, T.; Zhang, J. Investigating microclimate effects in an oasis-desert interaction zone. *Agr. Forest Meteorol.* **2020**, *290*, 107992. [CrossRef]
11. Xue, J.; Gui, D.; Lei, J.; Sun, H.; Zeng, F.; Mao, D.; Zhang, Z.; Jin, Q.; Liu, Y. Oasis microclimate effects under different weather events in arid or hyper arid regions: A case analysis in southern Taklimakan desert and implication for maintaining oasis sustainability. *Theor. Appl. Climatol.* **2019**, *137*, 89–101. [CrossRef]
12. Li, C.; Fu, B.; Wang, S.; Stringer, L.C.; Wang, Y.; Li, Z.; Liu, Y.; Zhou, W. Drivers and impacts of changes in China's drylands. *Nat. Rev. Earth Environ.* **2021**, *2*, 858–873. [CrossRef]
13. Li, Z.; Chen, Y.; Zhang, Q.; Li, Y. Spatial patterns of vegetation carbon sinks and sources under water constraint in Central Asia. *J. Hydrol.* **2020**, *590*, 125355. [CrossRef]
14. Ye, Z.; Chen, S.; Zhang, Q.; Liu, Y.; Zhou, H. Ecological Water Demand of Taitema Lake in the Lower Reaches of the Tarim River and the Cherchen River. *Remote Sens.* **2022**, *14*, 832. [CrossRef]
15. Ekwueme, B.; Agunwamba, J. Trend Analysis and Variability of Air Temperature and Rainfall in Regional River Basins. *Civ. Eng. J.* **2021**, *7*, 816–826. [CrossRef]
16. Gampe, D.; Zscheischler, J.; Reichstein, M.; Sullivan, O.M.; Smith, W.K.; Sitch, S.; Buermann, W. Increasing impact of warm droughts on northern ecosystem productivity over recent decades. *Nat. Clim. Chang.* **2021**, *11*, 772–779. [CrossRef]
17. Feng, S.; Fu, Q. Expansion of global drylands under a warming climate. *Atmos. Chem. Phys. Discuss.* **2013**, *13*, 14637–14665. [CrossRef]
18. Wang, Y.F.; Shen, Y.J.; Chen, Y.N.; Guo, Y. Vegetation dynamics and their response to hydroclimatic factors in the Tarim River Basin, China. *Ecohydrology* **2013**, *6*, 927–936. [CrossRef]
19. Xu, Z.; Fan, W.; Wei, H.; Zhang, P.; Ren, J.; Gao, Z.; Ulgiati, S.; Kong, W.; Dong, X. Evaluation and simulation of the impact of land use change on ecosystem services based on a carbon flow model: A case study of the Manas River Basin of Xinjiang, China. *Sci. Total Environ.* **2019**, *652*, 117–133. [CrossRef]
20. Hao, X.; Li, W.; Deng, H. The oasis effect and summer temperature rise in arid regions—Case study in Tarim Basin. *Sci. Rep* **2016**, *6*, 35418. [CrossRef] [PubMed]
21. Li, X.; Yang, K.; Zhou, Y. Progress in the study of oasis-desert interactions. *Agr. Forest Meteorol.* **2016**, *230–231*, 1–7. [CrossRef]
22. Xue, L.; Zhu, B.; Wu, Y.; Wei, G.; Liao, S.; Yang, C.; Wang, J.; Zhang, H.; Ren, L.; Han, Q. Dynamic projection of ecological risk in the Manas River basin based on terrain gradients. *Sci. Total Environ.* **2019**, *653*, 283–293. [CrossRef] [PubMed]
23. Gao, P.; Kasimu, A.; Zhao, Y.; Lin, B.; Chai, J.; Ruzi, T.; Zhao, H. Evaluation of the Temporal and Spatial Changes of Ecological Quality in the Hami Oasis Based on RSEI. *Sustainability* **2020**, *12*, 7716. [CrossRef]
24. Zhang, Z.; Xu, E.; Zhang, H. Complex network and redundancy analysis of spatial–temporal dynamic changes and driving forces behind changes in oases within the Tarim Basin in northwestern China. *Catena* **2021**, *201*, 105216. [CrossRef]
25. Pei, Z.; Fang, S.; Yang, W.; Wang, L.; Wu, M.; Zhang, Q.; Han, W.; Khoi, D.N. The Relationship between NDVI and Climate Factors at Different Monthly Time Scales: A Case Study of Grasslands in Inner Mongolia, China (1982–2015). *Sustainability* **2019**, *11*, 7243. [CrossRef]
26. Qi, S.; Li, X.; Duan, H. Oasis land-use change and its environmental impact in Jinta Oasis, arid northwestern China. *Environ. Monit. Assess.* **2007**, *134*, 313–320. [CrossRef] [PubMed]
27. Xie, Y.; Gong, J.; Sun, P.; Gou, X. Oasis dynamics change and its influence on landscape pattern on Jinta oasis in arid China from 1963a to 2010a: Integration of multi-source satellite images. *Int. J. Appl. Earth Obs.* **2014**, *33*, 181–191. [CrossRef]
28. Liu, Y.; Li, L.; Chen, X.; Zhang, R.; Yang, J. Temporal-spatial variations and influencing factors of vegetation cover in Xinjiang from 1982 to 2013 based on GIMMS-NDVI3g. *Global Planet. Chang.* **2018**, *169*, 145–155. [CrossRef]
29. Shi, G.; Ye, P.; Ding, L.; Quinones, A.; Li, Y.; Jiang, N. Spatio-Temporal Patterns of Land Use and Cover Change from 1990 to 2010: A Case Study of Jiangsu Province, China. *Int. J. Environ. Res. Public Health* **2019**, *16*, 907. [CrossRef] [PubMed]
30. Zhang, J.; Hao, X.; Hao, H.; Fan, X.; Li, Y. Climate Change Decreased Net Ecosystem Productivity in the Arid Region of Central Asia. *Remote Sens.* **2021**, *13*, 4449. [CrossRef]
31. Li, P.; Xu, L.; Liu, X.; Wu, P. Ecological security evaluation of an oasis in the north of the Tianshan Mountains based on three-dimensional ecological footprint model. *Arid Zone Res.* **2020**, *37*, 1337–1345. (In Chinese)
32. Leng, C.; Chen, Y.; Li, X.; Sun, Y. Evaluation of oasis stability in the lower reaches of the Tarim River. *J. Arid land* **2011**, *3*, 123–131. [CrossRef]
33. Wang, H.; Chen, Y.; Li, W. Hydrological extreme variability in the headwater of Tarim River: Links with atmospheric teleconnection and regional climate. *Stoch. Environ. Res. Risk Assess.* **2014**, *28*, 443–453. [CrossRef]

34. Zhang, Y.; An, C.; Liu, L.; Zhang, Y.; Lu, C.; Zhang, W. High Mountains Becoming Wetter While Deserts Getting Drier in Xinjiang, China since the 1980s. *Land* **2021**, *10*, 1131. [CrossRef]
35. Huang, J.; Wang, R.; Zhang, H. Analysis of patterns and ecological security trend of modern oasis landscapes in Xinjiang, China. *Environ. Monit. Assess.* **2007**, *134*, 411–419. [CrossRef] [PubMed]
36. Wang, F.; Chen, Y.; Li, Z.; Fang, G.; Li, Y.; Wang, X.; Zhang, X.; Kayumba, P.M. Developing a Long Short-Term Memory (LSTM)-Based Model for Reconstructing Terrestrial Water Storage Variations from 1982 to 2016 in the Tarim River Basin, Northwest China. *Remote Sens.* **2021**, *13*, 889. [CrossRef]
37. Fang, G.; Yang, J.; Chen, Y.; Li, Z.; Ji, H.; De, M. How Hydrologic Processes Differ patially in a Large Basin: Multisite and Multiobjective Modeling in the Tarim River Basin. *J. Geophys. Res. Atmos.* **2018**, *123*, 7098–7113.
38. Zhang, Q.; Chen, Y.; Li, Z.; Fang, G.; Xiang, Y.; Li, Y.; Ji, H. Recent Changes in Water Discharge in Snow and Glacier Melt-Dominated Rivers in the Tienshan Mountains, Central Asia. *Remote Sens.* **2020**, *12*, 2704. [CrossRef]
39. Chen, H.; Chen, Y.; Li, W.; Li, Z. Quantifying the contributions of snow/glacier meltwater to river runoff in the Tianshan Mountains, Central Asia. *Global Planet. Chang.* **2019**, *174*, 47–57. [CrossRef]
40. Duethmann, D.; Menz, C.; Jiang, T.; Vorogushyn, S. Projections for headwater catchments of the Tarim River reveal glacier retreat and decreasing surface water availability but uncertainties are large. *Environ. Res. Lett.* **2016**, *11*, 54024. [CrossRef]
41. Zhang, W.; Lu, Y.; Van Der Werf, W.; Huang, J.; Wu, F.; Zhou, K.; Deng, X.; Jiang, Y.; Wu, K.; Rosegrant, M.W. Multidecadal, county-level analysis of the effects of land use, Bt cotton, and weather on cotton pests in China. *Proc. Nat. Acad. Sci. USA* **2018**, *115*, E7700–E7709. [CrossRef] [PubMed]
42. Serbin, G.; Hunt, E.R.; Daughtry, C.S.T.; McCarty, G.W. Assessment of spectral indices for cover estimation of senescent vegetation. *Remote Sens. lett.* **2013**, *4*, 552–560. [CrossRef]
43. Wang, J.; Liu, D.; Ma, J.; Cheng, Y.; Wang, L. Development of a large-scale remote sensing ecological index in arid areas and its application in the Aral Sea Basin. *J. Arid Land* **2021**, *13*, 40–55. [CrossRef]
44. Shobairi, E.A. Dynamic estimation model of vegetation fractional coverage and drivers. *Int. J. Adv. Appl. Sci.* **2018**, *5*, 60–66. [CrossRef]
45. Li, F.; Chen, W.; Zeng, Y.; Zhao, Q.; Wu, B. Improving Estimates of Grassland Fractional Vegetation Cover Based on a Pixel Dichotomy Model: A Case Study in Inner Mongolia, China. *Remote Sens.* **2014**, *6*, 4705–4722. [CrossRef]
46. Zhao, T.; Yang, Y.; Mu, X. Monitoring Dynamic Changes of Vegetation Cover in the Tarim River Basin Based with Landsat Imagery and Google Earth Engine. In Proceedings of the IGARSS 2020—2020 IEEE International Geoscience and Remote Sensing Symposium, Waikoloa, HI, USA, 26 September–2 October 2020.
47. Li, Y.; Chen, Y.; Ye, Z.; Wang, F.; Sun, F.; Qin, J. Ecological responses of ecological water conveyance in the lower reaches of Tarim River for 20 years. *Arid Land Geogr.* **2021**, *44*, 700–707. (In Chinese)
48. Jiapaer, G.; Chen, X.; Bao, A. A comparison of methods for estimating fractional vegetation cover in arid regions. *Agr. Forest Meteorol.* **2011**, *151*, 1698–1710. [CrossRef]
49. Zeng, X.; Dickinson, R.; Walker, A.; Shaikh, M.; DeFries, R.; Qi, J. Derivation and Evaluation of Global 1-km Fractional Vegetation Cover Data for Land Modeling. *J. Appl. Meteorol.* **2000**, *39*, 826–839. [CrossRef]
50. Potter, C.; Klooster, S.; Genovese, V. Net primary production of terrestrial ecosystems from 2000 to 2009. *Clim. Chang.* **2012**, *115*, 365–378. [CrossRef]
51. Potter, C.S.; Randerson, J.T.; Field, C.B.; Matson, P.A.; Vitousek, P.M.; Mooney, H.A.; Klooster, S.A. Terrestrial ecosystem production; a process model based on global satellite and surface data. *Global Biogeochem. Cy.* **1993**, *7*, 811–841. [CrossRef]
52. Mann, H.B. Nonparametric tests against trend. *Econometrica* **1945**, *13*, 245–259. [CrossRef]
53. Kendall, M.G. *Rank Correlation Methods*; Springer: Boston, MA, USA, 1975.
54. Zhao, Y.; Zhang, H. Impacts of SST Warming in tropical Indian Ocean on CMIP5 model-projected summer rainfall changes over Central Asia. *Clim. Dynam.* **2016**, *46*, 3223–3238. [CrossRef]
55. Xu, M.; Kang, S.; Wu, H.; Yuan, X. Detection of spatio-temporal variability of air temperature and precipitation based on long-term meteorological station observations over Tianshan Mountains, Central Asia. *Atmos. Res.* **2018**, *203*, 141–163. [CrossRef]
56. Liu, S.; Ding, Y.; Shangguan, D.; Zhang, Y.; Li, J.; Han, H.; Wang, J.; Xie, C. Glacier retreat as a result of climate warming and increased precipitation in the Tarim river basin, northwest China. *Ann. Glaciol.* **2006**, *43*, 91–96. [CrossRef]
57. Xu, Y.; Yang, J.; Chen, Y. NDVI-based vegetation responses to climate change in an arid area of China. *Theor. Appl. Climatol.* **2016**, *126*, 213–222. [CrossRef]
58. Song, W.; Zhang, Y. Expansion of agricultural oasis in the Heihe River Basin of China: Patterns, reasons and policy implications. *Phys. Chem. Earth.* **2015**, *89–90*, 46–55. [CrossRef]
59. Yao, J.; Chen, Y.; Guan, X.; Zhao, Y.; Chen, J.; Mao, W. Recent climate and hydrological changes in a mountain–basin system in Xinjiang, China. *Earth-Sci. Rev.* **2022**, *226*, 103957. [CrossRef]
60. Tao, H.; Gemme, M.; Bai, Y.; Su, B.; Mao, W. Trends of streamflow in the Tarim River Basin during the past 50 years: Human impact or climate change? *J. Hydrol.* **2011**, *400*, 1–9. [CrossRef]
61. Shen, Y.; Shen, Y.; Fink, M.; Kralisch, S.; Sven, K.; Chen, Y.; Brenning, A. Trends and variability in streamflow and snowmelt runoff timing in the southern Tianshan Mountains. *J. Hydrol.* **2018**, *557*, 173–181. [CrossRef]

62. Duethmann, D.; Bolch, T.; Farinotti, D.; Kriegel, D.; Vorogushyn, S.; Merz, B.; Pieczonka, T.; Jiang, T.; Su, B.; Untner, G.A. Attribution of streamflow trends in snow and glacier melt-dominated catchments of the Tarim River, Central Asia. *Water Resour. Res.* **2015**, *51*, 4727–4750. [CrossRef]
63. Xiang, Y.; Chen, Y.; Zhang, Q.; Bian, W. Trends of snow cover and streamflow variation in Kaidu River and their influential factors. *Resour. Sci.* **2018**, *40*, 1855–1865. (In Chinese)
64. Li, B.; Chen, Y.; Chipman, J.W.; Shi, X. Why does the runoff in Hotan River show a slight decreased trend in northwestern China? *Atmos. Sci. Lett.* **2018**, *19*, e800. [CrossRef]
65. Ren, C.; Long, A.; Yu, J.; Yin, Z.; Zhang, J. Effects of climate and underlying surface changes on runoff of Yarkant River Source. *Arid Land Geogr.* **2021**, *44*, 1373–1383.
66. Ye, Z.; Liu, H.; Chen, Y.; Shu, S.; Wu, Q.; Wang, S. Analysis of water level variation of lakes and reservoirs in Xinjiang, China using ICESat laser altimetry data (2003–2009). *PLoS ONE* **2017**, *12*, e183800. [CrossRef]
67. Wang, X.; Liu, Q.; Liu, S.; Wei, J.; Jiang, Z. Heterogeneity of glacial lake expansion and its contrasting signals with climate change in Tarim Basin, Central Asia. *Environ. Earth Sci.* **2016**, *75*, 696. [CrossRef]
68. Zhang, L.; Wylie, B.K.; Ji, L.; Gilmanov, T.G.; Tieszen, L.L.; Howard, D.M. Upscaling carbon fluxes over the Great Plains grasslands: Sinks and sources. *J. Geophys. Res.* **2011**, *116*, G3.
69. Xiang, Y.; Wang, Y.; Chen, Y.; Bai, Y.; Zhang, L.; Zhang, Q. Hydrological Drought Risk Assessment Using a Multidimensional Copula Function Approach in Arid Inland Basins, China. *Water* **2020**, *12*, 1888. [CrossRef]
70. Xiang, Y.; Wang, Y.; Chen, Y.; Zhang, Q. Impact of Climate Change on the Hydrological Regime of the Yarkant River Basin, China: An Assessment Using Three SSP Scenarios of CMIP6 GCMs. *Remote Sens.* **2022**, *14*, 115. [CrossRef]
71. Chen, Y.; Zhang, X.; Fang, G.; Li, Z.; Wang, F.; Qin, J.; Sun, F. Potential risks and challenges of climate change in the arid region of northwestern China. *Reg. Sustain.* **2020**, *1*, 20–30. [CrossRef]
72. Ćosić-Flajsig, G.; Vučković, I.; Karleuša, B. An Innovative Holistic Approach to an E-flow Assessment Model. *Civ. Eng. J.* **2020**, *6*, 2188–2202. [CrossRef]
73. Amuti, T.; Luo, G. Analysis of land cover change and its driving forces in a desert oasis landscape of Xinjiang, northwest China. *Solid Earth* **2014**, *5*, 1071–1085. [CrossRef]
74. Zhou, D.; Luo, G.; Lu, L. Processes and trends of the land use change in Aksu watershed in the central Asia from 1960 to 2008. *J. Arid Land* **2010**, *2*, 157–166.
75. Zhang, P.; Deng, X.; Long, A.; Xu, H.; Ye, M.; Li, J. Change in Spatial Distribution Patterns and Regeneration of Populus euphratica under Different Surface Soil Salinity Conditions. *Sci. Rep.* **2019**, *9*, 9123. [CrossRef]
76. Ling, H.; Guo, B.; Yan, J.; Deng, X.; Xu, H.; Zhang, G. Enhancing the positive effects of ecological water conservancy engineering on desert riparian forest growth in an arid basin. *Ecol. Indic.* **2020**, *118*, 106797. [CrossRef]
77. Fu, L.; Zhang, L.; He, C. Analysis of Agricultural Land Use Change in the Middle Reach of the Heihe River Basin, Northwest China. *Int. J. Environ. Res. Public Health* **2014**, *11*, 2698–2712. [CrossRef] [PubMed]
78. Deng, H.; Chen, Y. Influences of recent climate change and human activities on water storage variations in Central Asia. *J. Hydrol.* **2017**, *544*, 46–57. [CrossRef]